Hittite Journal of Science and Engineering, 2018, 5 (2) 91-96
ISSN NUMBER: 2148-4171
DOI: 10.17350/HJSE19030000078

Mineralogical and Geochemical Characterization of Ancient Ceramic Sherds from Dipsizin Cave (Karaman, Turkey)

M. Yavuz HÜSEYİNCA[1] Osman DOĞANAY[2]
[1]Selçuk University, Department of Geological Engineering, Konya, TURKEY
[2]Aksaray University, Department of Archaeology, Aksaray, TURKEY

ABSTRACT

Raw materials of two ancient ceramic sherds (ceramic-1 and ceramic-2) from Dipsizin cave were analyzed by SEM-EDS in order to characterize ceramic fabrics. Characterization includes separation of temper and clay paste sections, qualitative determination of mineralogical compositions and percentage calculations of raw materials by region sketching. In this perspective, ceramic-1 is characterized as % 41.83 temper (quartz, albite, rutile, lime, organic material) and % 58.17 clay paste. Then, ceramic-2 is characterized to be % 37.52 temper (quartz, anorthoclase, rutile, lime, organic material) and % 62.48 clay paste. Clay paste sections of both ceramics include mixture of clay minerals belonging to illite and smectite clay groups. In comparison, percentages of temper and clay paste sections of ceramic-1 and ceramic-2 differ % 4.31 from each other and variety of raw materials making up both ceramic bodies are nearly same except feldspars. But individually quartz and lime percentages between ceramics differ nearly two times. In this opinion we realize that raw materials are mixed by tracking two recipes. These recipes can be explained by different pottery making technologies and/or different archaeological provenances.

Keywords:
Ceramic Sherd; Characterization; Dipsizin Cave; Region Sketching, Sarıveliler, SEM-EDS

Article History:
Received: 2017/05/05
Accepted: 2017/11/04
Online: 2018/04/06

***Correspondence to**: M. Yavuz Huseyinca, Selcuk University, Department of Geological Engineering, 42250, Konya, TURKEY*
E-Mail: yhuseyinca@selcuk.edu.tr
Phone: +90 332 223 2115
Fax: +90 332 241 0635

INTRODUCTION

Dipsizin Cave is located in the vicinity of Sarıveliler District of Karaman Province in Turkey (Figure 1). In ancient times the cave was located in Cilicia Region and to the south of Isauria Region (Figure 2) [1]. A strata of soil which contains remnants indicative of human usage is defined as cultural soil. The unique specification distinguishing Dipsizin Cave from its analogues in the Taurus Mountains is its cultural soil as it is found rarely in caves (Figure 3a, b). This soil includes numerous ceramic fragments and some of them giving date and form have been cataloged. Archaeological specifications of these ceramics indicate that they are brought from different regions into the cave and this cave was a temporary resting place or a shelter for caravans traveling between the ancient cities like Pharax, Zenonopolis, Lamos and Golgosos [2].

In this study raw materials of ceramic-1 (C-1) and ceramic-2 (C-2) (Figure 4a, b) from the catalog were investigated for characterization under the perspective of "provenance studies involve characterization of ancient ceramics" [3]. Raw materials used for pottery making can be categorized into three parts; clays, tempers and glazes. Clay, which is the dominant constituent plays most important role with two properties. First is the plasticity for taking shape before firing and the second is conservation of its shape while and after firing. Chemically, clays are hydrous aluminum silicates, usually containing minor amounts of impurities such as K, Na, Ca, Mg or Fe [4, 5]. There are three major clay mineral groups (kaolinite, illite and smectite) and they have chemically distinct compositions. However most ancient pottery was made from a mixture of these clay groups.

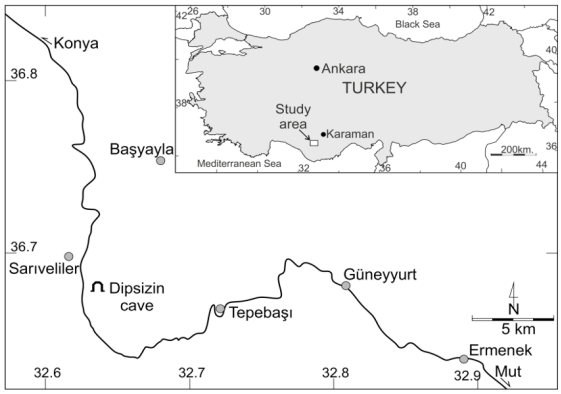

Figure 1. Geographic location of Dipsizin Cave

Figure 2. Settlement around Dipsizin Cave in ancient ages

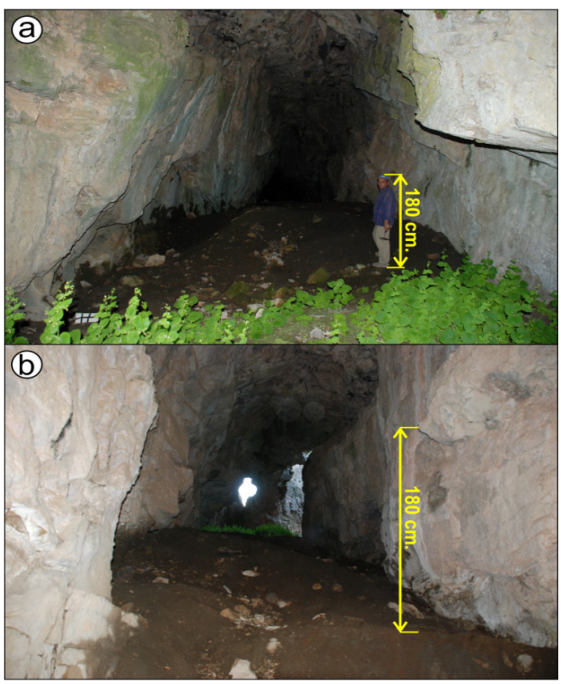

Figure 3. Photographs showing interior **(a)** and entrance **(b)** of Dipsizin cave

Some clays are suitable for potting and straightly dug from the deposit but some have to be mixed as they are not plastic enough or too plastic [6]. Tempers are additives mixed in order to reduce shrinkage of the final product and to improve workability of the clay paste. A wide variety of raw materials

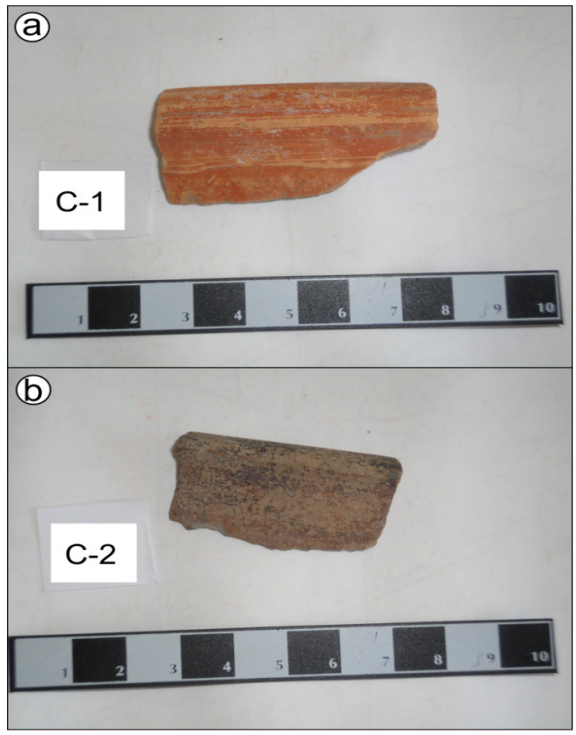

Figure 4. Catalog photographs of C-1 **(a)** and C-2 **(b)**

such as quartz sand, fossil shells, calcite, mica, crushed rock, and organic materials can be used as a temper [7, 8]. Glazes are glassy coatings melted on the surface of the pottery to make them waterproof and to give decorative features. All glazes are consist of mainly silica and some flux agents. The color of the glaze directly depends on the type of the flux agent and the firing temperature of the pot [6].

This study aims to define above mentioned raw materials and their percentages used in obtained ceramics by applying non-destructive methods. This procedure will help to determine producing technologies and/or archaeological provenances of the ceramics which play important role in archaeology.

GEOLOGICAL FRAMEWORK

Dipsizin Cave is geographically located in the Central Taurus Mountains which is part of the Taurus orogenic belt. This belt is composed of several tectonic rock slices (namely Bolkardağı, Aladağ, Geyikdağı, Alanya, Bozkır and Antalya) so that they have long tectonic contacts with each other and reflect different basin conditions [9-12]. General lithology of these rocks deposited in the Cambrian - Eocene age interval include metamorphosed carbonates, clastics and ophiolitic rocks. In the central part of the Taurus Belt, basement rocks are unconformably overlaid by the post-Eocene aged Mut Basin deposits which include horizontally bedded clastics and carbonates [13, 14]. Formation of Dipsizin cave within the metacarbo-

nates of the basement rocks can be explained by karstic dissolution mechanism.

MATERIAL AND METHODS

This work is focused on the application of Scanning Electron Microscopy (SEM) and Energy Dispersive Spectroscopy (EDS) techniques to C-1 and C-2 obtained from Dipsizin cave. SEM is a high magnification microscope which the image is generated by the interaction of generated high energy electrons and sample atoms. With it, EDS is a micro-analytical technique conventionally used in SEM for the local determination of chemical elements in solid samples [15]. In this technique a special energy-sensitive detector adapted to SEM receives the generated X-rays and sorts them according to energy. A computer software analyzes the spectrum and looks for characteristic peaks indicative of certain elements. Besides determining elemental composition of individual points on the sample, EDS analysis can be used to map out the lateral distribution of elements from the imaged area. These maps can give accurate results of relative element proportions to understand the material properties [16]. On the overall the EDS microanalysis is regarded as a non-destructive technique and applied to many problems of archaeological ceramics [17-21].

In the study, the samples were bombarded with high energy electrons produced by tungsten filament emitter under accelerating voltage of 15 keV in SEM-EDS. Element distribution (ED) map images of silicon (Si), titanium (Ti), sodium (Na), carbon (C), calcium (Ca), aluminum (Al), potassium (K), oxygen (O), magnesium (Mg) and iron (Fe) are taken under the magnification level of 400X. Then each ceramic fabric is investigated under the sections of temper and clay paste. Sections are separated according to the grain size contrast between them. Noticeable contrast indicates manual addition of temper to clay [8]. After separation process, element distribution (ED) maps, EDS analysis and compositions of standard minerals are evaluated for mineralogical considerations. Region sketches and percentages are obtained from image analyzing software (Image-Pro).

RESULTS AND DISCUSSION

An ED map specifies a single element content and distribution in the defined area with a color code. Colors of ED maps are assigned automatically by the computer to a single chemical element. Accordingly, the total element content in the defined area is separated to numerous single element maps. On the contrary to this definition, starting from the induction method our theory is to arrive at the total element content in that area by the proper combination of each element map. To do this, element maps are manually placed on top of each other to search for overlapping in colors. Then it is found out which elements constitute the areas where the overlaps occur. In the next step mineralogy is determined by comparing the found element association with the contents of proper EDS points and known minerals. Defining mineralogy is important step for calculating raw material percentages which is valuable for evaluating production technologies of ceramics. In this concept characterizations of C-1 and C-2 are explained under separate titles.

Characterization of C-1

SEM secondary electron image (SEI) and backscattered electron image (BEI) with EDS locations are shown in Figure 5a, b. SE and BE images help to understand surface topography and element distribution of the scanned area respectively [19]. Color coded ED maps of Si (white), Ti (blue), Na (turquoise), C (red), Ca (purple), Al (cyan), K (brown), O (green), Mg (violet) and Fe (olive) are also shown in Figure 5c- l. High brightness of a color indicates a high concentration of related element or vice versa. The black color means no concentration of related element in the map [15].

To find qualitative composition of white colored regions in ED map of Si (Figure 5c) we superpose other ED maps for overlapping colors. Then we conclude that there is only green colored regions in O map (Figure 5j) indicating Si and O are the main constituents of our white regions. For mineralogical determination, beside proper overlapping in ED maps we look for a mineral whose chemical composition is close to point 5a (Table 1) in terms of defined element variety. In this concept quartz mineral (% 46.74 Si) has very close composition to point 5a (% 45.72 Si) and suggest that our white colored regions are quartz. Distribution of Na concentration is represented by the turquoise colored regions in ED map (Figure 5e). When manually superposed, colors overlapped with the mentioned regions belong to Al, Si and O maps (Figure 5h, c, j). Therefore, our candidate mineral qualitatively includes Na, Al, Si and O elements. In order to identify this mineral, the similarity between the quantitative compositions of point 2a (% 6.82 Na, % 10.89 Al and % 32.92 Si) and a mineral with standard formula is compared in terms of defined elements. Here, albite (% 8.77 Na, % 10.29 Al and % 32.13 Si) is suggested which has closest content to 2a point (Table 1). Ti concentration is represented by blue colored regions in ED map (Figure 5d). When superposed, overlapping colors with related regions are only in O map (Figure 5j) indicating that our mineral contains Ti and O elements. Comparison between point 9a (% 58.80 Ti and % 0.86 Fe) in Table 1 and rutile content (% 58.43 Ti and % 1.83 Fe) verifies similarity of contents and suggest that our blue colored grains are rutile. We know that rutile is stable in

Table 1. Chemical compositions of points 1a to 10a (wt%) for C-1.

Element/ Point	C	O	Na	Mg	Al	Si	K	Ca	Ti	Fe	Sum
1a	3.20	43.91	7.35	0.00	10.89	32.92	0.44	0.19	0.31	0.78	99.99
2a	0.00	47.56	6.82	0.10	11.08	33.84	0.12	0.21	0.00	0.00	99.73
3a	9.70	41.15	0.00	4.79	10.39	20.82	1.89	1.45	1.02	8.79	100.00
4a	9.25	41.40	0.44	1.16	16.51	23.24	4.26	1.17	0.27	2.28	99.98
5a	6.56	46.32	0.21	0.04	0.65	45.72	0.00	0.11	0.11	0.25	99.97
6a	77.86	12.08	0.45	0.26	0.74	1.55	0.08	0.00	0.00	0.00	93.02
7a	12.05	37.00	0.60	0.23	10.11	28.00	8.87	0.78	0.41	1.79	99.84
8a	12.17	43.53	0.12	0.25	9.64	13.64	0.44	17.81	0.16	2.01	99.77
9a	4.35	31.79	0.27	0.18	1.26	1.83	0.34	0.29	58.80	0.86	99.97
10a	6.09	43.21	0.00	2.87	10.67	17.33	1.02	1.30	1.11	16.35	99.95

most weathering environments and generally can mix with clay [22-24]. Ca content is shown by purple colored regions in ED map (Figure 5g). When superposed, green color of O map overlaps with these regions. So, element variety includes Ca and O but not C. Therefore our purple colored and pellet shaped regions should be lime rather than grounded calcium carbonate ($CaCO_3$). C distribution is represented by red colored regions in ED map (Figure 5f). When superposed there is no other element color overlapping with these regions. Mono elemental variety and high C (% 77.86) content in point 6a (Table-1) suggest that these regions should be organic material. Organic material can be found with clay naturally or can be added to mixture by pottery maker in order to improve plasticity and firing conditions [6].

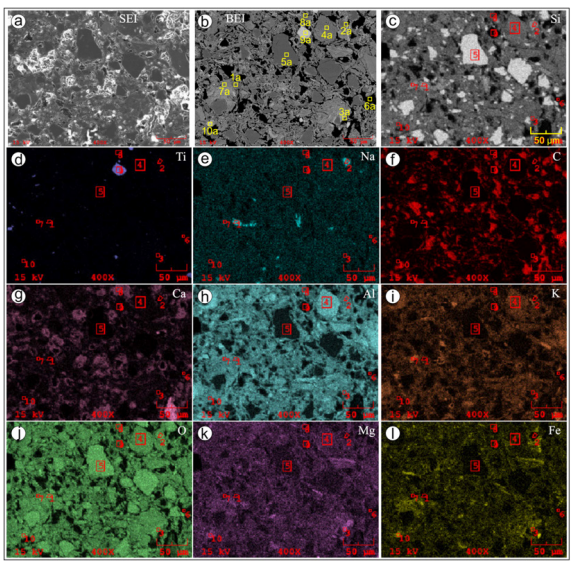

Figure 5. SEI **(a)**, BEI adapted with EDS locations **(b)** and ED maps of Si **(c)**, Ti **(d)**, Na **(e)**, C **(f)**, Ca **(g)**, Al **(h)**, K **(i)**, O **(j)**, Mg **(k)** and Fe **(l)** for C-1

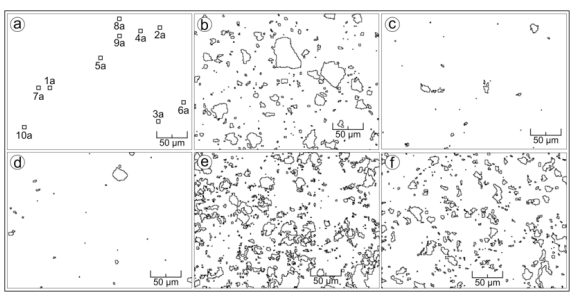

Figure 6. SEI **(a)**, EDS locations of points 1a to 10a **(a)** and region sketches of quartz **(b)**, albite **(c)**, rutile **(d)**, lime **(e)** and organic material **(f)** for C-1

Accordingly, temper section of C-1 is composed of quartz (SiO_2), albite ($NaAlSi_3O_8$), rutile (TiO_2), lime (CaO) and organic material. Percentages of these constituents are calculated as % 12.00, % 0.73, % 0.85, % 18.10 and % 10.15 respectively and summed to % 41.83 according to image analysis (Figure 6). Above mentioned raw materials are all included into the temper section as they are not clay in mineralogy. Finally, C-1 is characterized to be % 41.83 temper and remaining % 58.17 clay paste.

To determine clay paste section remained from the temper section we obtain proper overlapping of Al, Si and O elements as clays are hydrous aluminum silicates. After verifying this we see that overlapping of K, Mg and Fe occurs too (Figure 5i, k, l). These are probably impurities that can take place in clay minerals. Especially, K prefers mainly illite group [25], whilst Mg and Fe prefer smectite group clay minerals [5]. Therefore clay section of C-1 seems to be the mixture of clay minerals belonging to illite and smectite group.

Characterization of C-2

SEI, BEI including EDS locations and color coded ED maps of Si (white), Ti (turquoise), Na (blue), C (red), Ca (brown), Al (cyan), K (magenta), O (green), Mg (violet) and Fe (olive) belonging to C-2 are shown in Figure 7a, l. Chemical compositions of points 1b to 10b are also shown in Table 2. Separation of temper and clay paste sections, identification of minerals and percentage calculations within C-2 are performed as done in C-1.

White colored regions in Si map (Figure 7c) overlap only with green colors of O map (Figure 7j) indicating that these regions include Si and O elements. Consistency between quantitative compositions of point 5b (% 44.77 Si) in

Table 2. Chemical compositions of points 1b to 10b (wt%) for C-2.

Element/ Point	C	O	Na	Mg	Al	Si	K	Ca	Ti	Fe	Sum
1b	64.07	17.95	0.23	0.18	2.67	12.84	0.69	0.67	0.27	0.00	99.57
2b	9.45	41.77	5.49	0.13	9.88	28.66	2.72	0.33	0.25	0.99	99.67
3b	7.94	42.15	0.00	5.60	11.26	20.19	0.50	0.75	0.31	11.06	99.76
4b	9.24	39.63	0.54	0.25	20.48	23.71	3.55	0.41	0.15	1.69	99.65
5b	6.72	46.75	0.09	0.06	0.64	44.77	0.07	0.16	0.01	0.24	99.51
6b	0.00	41.27	0.72	1.32	3.10	27.59	2.62	3.01	0.00	0.00	79.63
7b	12.60	38.77	0.36	0.08	9.46	29.32	7.69	0.00	0.26	1.33	99.87
8b	3.62	44.26	0.45	0.88	12.02	20.42	1.65	14.23	1.23	0.00	98.76
9b	3.02	40.97	0.17	0.60	8.07	14.13	1.49	0.40	25.81	5.21	99.87
10b	6.69	41.45	0.13	3.93	13.12	16.54	1.36	0.80	1.17	14.37	99.56

Table 2 and quartz (% 46.74 Si) suggest that our regions are quartz grains. Blue colored regions in Na map overlaps with Al, Si and K elements when superposed (Figure 7e, h, c, i). So, Na, Al, Si and K elements are main constituents of blue colored regions. Consistency between chemical compositions of point 2b (% 5.49 Na, % 2.72 K, % 9.88 Al and % 28.66 Si) and anorthoclase (% 5.45 Na, % 2.47 K, % 11.71 Al and % 29.35 Si) suggest that these regions are anorthoclase grains. Turquoise colored regions in Ti map overlap only with O (Figure 7d, j). So, chemical variety include Ti and O for the candidate mineral. Close chemical compositions of point 9b (Table 2) and rutile suggest that mentioned regions could be rutile. Brown colored regions in Ca map overlap with green color of O map (Figure 7g, j) but don't with C map indicating that these pellet shaped regions are lime rather than grounded limestone. C distribution is represented by red colored regions in ED map (Figure 7f). High C content of point 1b (% 64.07) in Table 2 and no overlapping of any element with these regions indicate organic material origin.

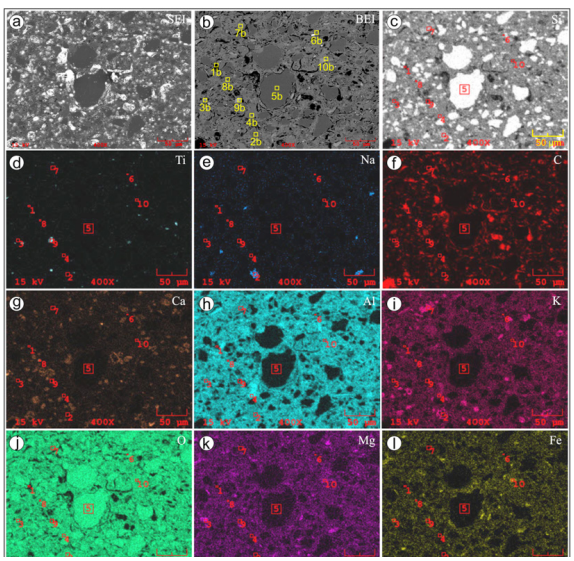

Figure 7. : SEI **(a)**, BEI adapted with EDS locations **(b)** and ED maps of Si **(c)**, Ti **(d)**, Na **(e)**, C **(f)**, Ca **(g)**, Al **(h)**, K **(i)**, O **(j)**, Mg **(k)** and Fe **(l)** for C-2

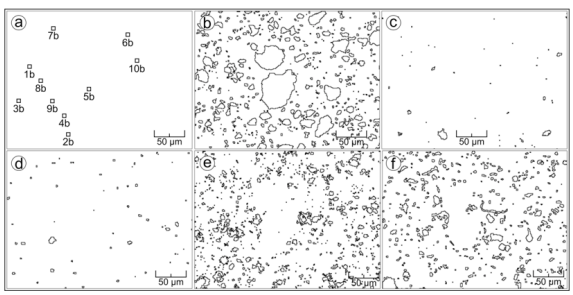

Figure 8. : EDS locations of points 1b to 10b **(a)** and region sketches of quartz **(b)**, anorthoclase **(c)**, rutile **(d)**, lime **(e)** and organic material **(f)** for C-2

Accordingly, temper section of C-2 is composed of quartz (SiO_2), anorthoclase ($K,NaAlSi_3O_8$), rutile (TiO_2), lime (CaO) and organic material. Percentages of these constituents are calculated as % 20.10, % 0.55, % 0.62, % 8.25 and % 8.00 respectively and summed to % 37.52 according to region sketches (Figure 8). Then C-2 is characterized to be % 37.52 temper and remaining % 62.48 clay paste section.

In clay paste section of C-2 we see overlapping of Al, Si and O elements indicating clay mineral existence. We see also overlapping of K, Mg and Fe (Figure 7i, k, l) which could be evaluated as impurities in clay minerals. As a result we can suggest that clay paste section of C-2 is a mixture of clay minerals belonging to illite and smectite groups as in C-1.

CONCLUSION

As a result of the study, following items can be arranged:

1- C-1 is characterized as % 41.83 temper (quartz, albite, rutile, lime, organic material) and % 58.17 clay paste. Also, C-2 is characterized to be % 37.52 temper (quartz, anorthoclase, rutile, lime, organic material) and % 62.48 clay paste.

2- When compared, percentages of temper and clay paste sections in C-1 and in C-2 seem to be close in % 4.31 vicinity. But individually quartz and lime percentages of C-1 (% 12.00 quartz and % 18.10 lime) and C-2 (% 20.10 quartz and % % 8.25 lime) differ nearly two times from each other. Noticeable diversity in percentages of quartz and lime sug-

gest that these raw materials are mixed following different recipes indicative of different production technologies and/or two distinct pottery makers within the meaning of different archaeological provenance.

3- In comparison, temper sections of both C-1 and C-2 have nearly same qualitative compositions except C-1 have albite and C-2 have anorthoclase.

4- Clay paste sections of ceramics both reflect mixture of clay minerals belonging to illite and smectite groups.

5- Similarity between the varieties of raw materials indicate common or close geological provenance.

6- Grain size contrast of quartz and pellet shaped structure of lime in both ceramic textures indicate manual addition of these.

7- Low percentages of feldspars and rutile indicate that they are not manually added.

8- High organic material content may indicate direct input of clay from a lake deposit or manual addition of it to improve plasticity of the mixture [6].

9- Percentage calculation of raw materials can give important data for characterization of ancient ceramics and behavior of pottery makers.

10- We suggest that characterization of ceramics could be done non-destructively by the procedure applied in this study.

ACKNOWLEDGMENTS

The authors thank the editor and anonymous reviewers for their constructive comments to the manuscript.

References

1. Heinrich, K, Asia citerior, in: David Rumsey historical map collection, Dietrich Reimer, Berlin, 1903.
2. Doğanay, O, Duman, B. Isauria bölgesi'nden bir grup seramik: Adiller Dipsizin mağarası, in: Ş. Dönmez (Ed.) Sümer Atasoy'a armağan yazılar, Hel Yayınları, Ankara, pp. 83–94, 2013.
3. Tite, MS. The impact of electron microscopy on ceramic studies. Proceedings of the British Academy 77 (1992) 111–131.
4. Guggenheim, S, Martin, RT. Definition of clay and clay mineral: Joint report of the AIPEA nomenclature and CMS nomenclature committees. Clays and Clay Minerals 43 (1995) 255–256.
5. Mukherjee, S. The science of clays, Springer Netherlands, India, 2013.
6. Rapp, G. Archaeomineralogy, second ed. Springer, Berlin Heidelberg, 2009.
7. Shepard, AO. Ceramics for the archaeologist, Carnegie institution, Washington, 1956.
8. Dickinson, WR. Petrographic temper provinces of prehistoric pottery in Oceania. Records of the Australian Museum 50 (1998) 263–276.
9. Özgül, N. Torosların bazı temel jeolojik özellikleri. Türkiye Jeoloji Kurumu Bülteni 19 (1976) 65–78.
10. Özgül, N. Bozkır–Hadim–Taşkent (Orta Toroslar'ın kuzey kesimi) dolayında yer alan tektono–stratigrafik birliklerin stratigrafisi. Maden Tetkik ve Arama Dergisi 119 (1997) 113–174.
11. Özgül, N, Arpat, E. Structural units of Taurus orogenic belt and their continuation in the neighbouring regions. Geological Society of Greece Bulletin 10 (1973) 156–164.
12. Gutnic, M, Monod, O, Poisson, A, Dumont, JF. Geeologie des Taurides occidentales (Turquie), Societe Geologique de France, Paris, 1979.
13. Gedik, A, Birgili, Ş, Yılmaz, H, Yoldaş, R. Mut–Ermenek–Silifke Yöresinin Jeolojisi ve Petrol Olanakları. Türkiye Jeoloji Kurumu Bülteni 22 (1979) 7–26.
14. Bassant, P, Van Buchem, FSP, Strasser, A, Görür, N. The stratigraphic architecture and evolution of the Burdigalian carbonate–siliciclastic sedimentary systems of the Mut Basin, Turkey. Sedimentary Geology 173 (2005) 187–232.
15. Reed, SJB. Electron microprobe analysis and scanning electron microscopy in geology, Cambridge University Press, U.K., 2005.
16. Goldstein, JI, Newbury, DE, Echlin, P, Joy, DC, Fiori, C, Lifshin, E. Scanning electron microscopy and X–Ray microanalysis, Plenum Publishing, New York, 1981.
17. Tite, MS, Freestone, IC. The use of scanning electron microscopy in the technological examination of ancient ceramics, in: J.S. Olin, A.D. Franklin (Eds.) Archaeological Ceramics, Smithsonian Institution Press, Washington, pp. 109–120, 1982.
18. Freestone, IC, Middletonand, AP. Mineralogical applications of the analytical SEM in archaeology. Mineralogical Magazine 51 (1987) 21–31.
19. Froh, J. Archaeological ceramics studied by scanning slectron microscopy. Hyperfine Interactions 154 (2004) 159–176.
20. Laviano, R, Muntoni, IM. Provenance and technology of Apulian Neolithic pottery, in: M. Maggetti, B. Messiga (Eds.) Geomaterials in Cultural Heritage Geological Society Special Publications, London, pp. 49–62, 2006.
21. Wassilkowska, A, Czaplicka–Kotas, A, Zielina, M, Bielski, A. An analysis of the elemental composition of micro–samples using EDS technique. Technical Transactions 1 (2014) 133–148.
22. Morton, AC. Stability of detrital heavy tertiary sandstones from the north sea basin. Clay minerals 19 (1984) 287–308.
23. Pettijohn, FJ, Potter, PE, Siever, R. Sand and Sandstone, Springer New York, 1987.
24. Force, ER. Geology of titanium–mineral deposits, Geological Society of America, U.S.A, 1991.
25. Cox, R, Lowe, DR, Cullers, RL. The influence of sediment recycling and basement composition on evolution of mudrock chemistry in the southwestern United States. Geochimica et Cosmochimica Acta 59 (1995) 2919–2940.